THE JOURNAL OF BIOLOGICAL CHEMISTRY VOL. 286, NO. 9, pp. 7348–7358, March 4, 2011
Printed in the U.S.A.

# Sphingosine-1-phosphate Lyase Deficiency Produces a Pro-inflammatory Response While Impairing Neutrophil Trafficking*[S]

Received for publication, August 3, 2010, and in revised form, December 15, 2010 Published, JBC Papers in Press, December 20, 2010, DOI 10.1074/jbc.M110.171819

**Maria L. Allende[‡1], Meryem Bektas[‡1], Bridgin G. Lee[‡], Eliana Bonifacino[‡], Jiman Kang[‡], Galina Tuymetova[‡], WeiPing Chen[§], Julie D. Saba[¶], and Richard L. Proia[‡2]**

*From the [‡]Genetics of Development and Disease Branch and the [§]Microarray Core Laboratory, NIDDK, National Institutes of Health, Bethesda, Maryland 20892 and the [¶]Children's Hospital Oakland Research Institute (CHORI), Oakland, California 94609*

**Sphingosine-1-phosphate (S1P) lyase catalyzes the degradation of S1P, a potent signaling lysosphingolipid. Mice with an inactive S1P lyase gene are impaired in the capacity to degrade S1P, resulting in highly elevated S1P levels. These S1P lyase-deficient mice have low numbers of lymphocytes and high numbers of neutrophils in their blood. We found that the S1P lyase-deficient mice exhibited features of an inflammatory response including elevated levels of pro-inflammatory cytokines and an increased expression of genes in liver associated with an acute-phase response. However, the recruitment of their neutrophils into inflamed tissues was impaired and their neutrophils were defective in migration to chemotactic stimulus. The IL-23/IL-17/granulocyte-colony stimulating factor (G-CSF) cytokine-controlled loop regulating neutrophil homeostasis, which is dependent on neutrophil trafficking to tissues, was disturbed in S1P lyase-deficient mice. Deletion of the S1P4 receptor partially decreased the neutrophilia and inflammation in S1P lyase-deficient mice, implicating S1P receptor signaling in the phenotype. Thus, a genetic block in S1P degradation elicits a pro-inflammatory response but impairs neutrophil migration from blood into tissues.**

Sphingosine 1-phosphate (S1P)[3] is a sphingolipid signaling molecule that exerts important physiologic functions through its interaction with a family of G protein-coupled receptors (S1P1–5) (1–4). S1P is synthesized by the phosphorylation of sphingosine by either of two sphingosine kinases, Sphk1 and Sphk2 (5, 6). After its formation, S1P may be either dephosphorylated back to sphingosine by the action of two specific S1P phosphatases, Sgpp1 and Sgpp2, or permanently degraded by the S1P lyase Sgpl1 to the nonsphingolipid substrates hexadecenal and phosphoethanolamine (7). Alternatively, S1P can be exported out of the cell where it is able to interact with the S1P receptors (5, 8).

S1P is found highly enriched in the circulation-in both blood and lymph-while its concentration in tissues remains very low by comparison, as the result of the combined synthetic and degradative activities involved in the S1P biosynthetic pathway (9). Blood S1P is produced by erythrocytes (10–12), but other cells such as mast cells and platelets can also secrete S1P (13, 14). Endothelial cells can contribute to the circulating S1P pool (15, 16) and are likely responsible for the S1P that is present in the lymph (12).

The proper compartmentalization of S1P in circulation and in tissues is important for the trafficking and positioning of lymphocytes. The egress of lymphocytes out of primary and secondary lymphoid organs is dependent on S1P receptors on lymphocytes (17–23), which recognize the higher concentrations of S1P around exit points leading to the blood and lymph (12, 24, 25). When the activity of S1P lyase is inhibited or deleted as in the S1P lyase-knock-out ($Sgpl1^{-/-}$) mice, compartmental S1P concentrations are altered, blocking lymphocyte egress and resulting in lymphophenia (24, 26, 27).

In S1P lyase-deficient mice, neutrophils are highly elevated in blood, in contrast to their low lymphocyte numbers (26). Here we report that the S1P lyase-null mice have an elevated pro-inflammatory response with impaired migration of neutrophils into tissues resulting in an abnormal neutrophil homeostatic regulatory loop. These results implicate S1P lyase activity as a regulator of inflammatory responses and neutrophil trafficking.

## EXPERIMENTAL PROCEDURES

*Mice—*$Sgpl1^{-/-}$ mice were obtained from Philip Soriano, Mount Sinai School of Medicine, New York, and have been described previously (28, 29). LysMcre mice, $S1pr4^{+/-}$ mice and $Tlr4^{-/-}$ mice were obtained from The Jackson Laboratory, Bar Harbor, ME. The $Sgpl1^{-/-}$ and control $Sgpl1^{+/+}$ mice were generated from $Sgpl1^{+/-}$ matings. To specifically delete the S1P1 receptor from granulocytes and macrophages, we established $S1Pr1^{fl/fl}$ mice (30) carrying a lysozyme promoter-driven *Cre* recombinase transgene (Gr-*S1pr1*KO mice) derived from LysMcre mice (31). The following double

* This research was supported, in whole or in part, by the Intramural Research Program of the National Institutes of Health, NIDDK by Public Health Service Grant CA77528 (to J. D. S.) and National Institutes of Health Grant C06 RR018823 (to the Medical University of South Carolina Lipomics Core).

[S] The on-line version of this article (available at http://www.jbc.org) contains supplemental Figs. S1–S8.

[1] Both authors contributed equally to this work.

[2] To whom correspondence should be addressed: NIDDK, National Institutes of Health, Bethesda, MD 20892. Tel.: 301-496-4391; Fax: 301-496-0839; E-mail: proia@nih.gov.

[3] The abbreviations used are: S1P, sphingosine-1-phosphate; DKO, double knockout; P6, postnatal day 6; P18, postnatal day 18; RT-qPCR, real-time-quantitative PCR; APC, allophycocyanin; PerCP, peridinin chlorophyll protein; PE, phycoerythrin; MCP, monocyte chemoattractant protein; G-CSF, granulocyte-colony stimulating factor; GO, gene ontology; CBA, Cytometric Bead Array; MFI, mean fluorescence intensity.

knock-out (DKO) mice were produced through cross-breeding: *Sgpl1*$^{-/-}$ Gr-*S1pr1*KO, *Sgpl1*$^{-/-}$ *S1pr4*$^{-/-}$ and *Sgpl1*$^{-/-}$ *Tlr4*$^{-/-}$. Because *Sgpl1*$^{-/-}$ mice die around 3 to 5 weeks of age (26, 28, 29), all mice were analyzed at postnatal day 18 (P18) unless specified. Mice were housed in a clean conventional facility that excluded specific mouse pathogens. Mice were genotyped by multiplex PCR from tail snips using the set of primers and conditions for each mouse line listed below. ***Sgpl1***: 5′-CGCTCAGAAGGCTCTGAGTCATGG-3′, 5′-CATCAAGGAAACCCTGGACTACTG-3′, 5′-CCAAGTGTACCTGCTAAGTTCCAG-3′; conditions were previously described (29). ***S1pr1***$^{loxP}$: 5′-GAGCGGAGGAAGTTAAAAGTG-3′, 5′-CCTCCTAAGAGATTGCAGCAA-3′; conditions were previously described (30). ***Cre*****:** 5′-GCCTGCATTACCGGTCGATGC-3′, 5′-CAGGGTGTTATAAGCAATCCC-3′; the following conditions were used: denaturation, 94 °C × 5 min; amplification, 94 °C × 1 min, 60 °C × 1 min, 72 °C × 1 min (35 cycles); extension, 72 °C × 3 min. The Cre allele produces a band of about 500 bp. ***S1pr4***: 5′-CCCCGTAGAGGCTCAGGATAGCCAC-3′, 5′-GGCCTACGTGGTCAACGTGCTGC-3′. 5′-GACGAGTTCTTCTGAGGGGATCGATC-3′; the following conditions were used: denaturation, 94 °C × 5 min; amplification, 94 °C × 1 min, 60 °C × 30 s, 72 °C × 1.5 min (35 cycles); extension, 72 °C × 2 min. The *S1pr4*$^{+/+}$ allele produces a band of about 380 bp and the *S1pr4*$^{-/-}$ allele produces a band of 600 bp. ***Tlr4*****:** 5′-CAGGGTTGTACTTTAGGAGAGAGAGAAAGC-3′, 5′-GCTGCCCGGATCATCCAGG-3′, 5′-CCACCCATATTGCCTATACTCATTAGTTG-3′, 5′-GCCATGCCATGCCTTGTCTTCA-3′; the following conditions were used: denaturation, 95 °C × 10 min; amplification, 95 °C × 30 s, 57 °C × 1 min, 72 °C × 1 min (40 cycles); extension, 72 °C × 7 min. The *Tlr4*$^{+/+}$ allele produces a band of about 410 bp and the *Tlr4*$^{-/-}$ allele produces a band of 290 bp.

*Bone Marrow Transplantation*—Total bone marrow cells were isolated from *Sgpl1*$^{+/+}$ and *Sgpl1*$^{-/-}$ mice by flushing the femur and tibia from both legs two times with 1 ml of PBS. Cells were injected i.v. into lethally irradiated *Rag2*$^{-/-}$ mice (Taconic, Germantown, NY). Transplanted mice were analyzed 8 weeks after the procedure.

*LPS Treatment—Sgpl1*$^{+/+}$, and *Sgpl1*$^{-/-}$ mice were injected intraperitoneal with 10 mg/kg of body weight of LPS from *Escherichia coli* 055:B5 (Sigma-Aldrich) and observed for 5 days. In other experiments, mice were euthanized 60, 90, and 120 min after LPS injection.

*Thioglycollate-induced Peritonitis—Sgpl1*$^{+/+}$ and *Sgpl1*$^{-/-}$ mice were injected intraperitoneal with 300 $\mu$l of 4% thioglycollate (Sigma-Aldrich). After 4 h, mice were euthanized and blood collected by heart puncture. Cells that were recruited into the peritoneal cavity were collected by lavage using 1 ml of ice-cold PBS three times.

*Leukocyte Preparation*—Total bone marrow cells were isolated from mice by flushing the femur and tibia from both legs two times with 1 ml of PBS. To obtain total leukocytes, spleen and mesenteric lymph nodes were dissected and mechanically disaggregated. Single-cell suspensions were obtained using a 40-$\mu$m cell strainer. Peripheral blood was obtained by cardiac puncture. Red blood cells were removed from blood samples and splenic single-cell suspensions by ammonium chloride lysis. For some experiments, neutrophils were sorted from total bone marrow cells using anti-Ly-6G magnetic microbeads (Miltenyi Biotec, Auburn, CA). The absolute number of each cell subpopulation was determined by flow cytometry using CALTAG counting beads (Invitrogen, Carlsbad, CA). For bone marrow and spleen, the absolute cell counts were normalized by the individual body weight expressed in grams. Alternatively, blood cell counts were determined in the Department of Laboratory Medicine at the National Institutes of Health.

*Histological Analysis*—Tissues from *Sgpl1*$^{+/+}$ and *Sgpl1*$^{-/-}$ mice were fixed and embedded in paraffin. Sections were stained with H&E. A comprehensive histologic evaluation of the sections was performed by the National Institutes of Health Division of Veterinary Resources Pathology Service.

*Flow Cytometry*—Cells were diluted in 1% BSA-PBS and incubated with anti-Fc$\gamma$R antibody (BD Biosciences, San Jose, CA) to block binding of conjugated antibodies to Fc$\gamma$R (BD Biosciences). Antibodies anti-mouse Gr-1 (FITC- and allophycocyanin [APC]-conjugated), anti-CD11b (phycoerythrin (PE)- and FITC-conjugated), anti-CD4 (peridinin chlorophyll protein [PerCP]-conjugated), anti-CD8 (PE-conjugated), anti-B220 (APC-conjugated), anti-CD62L (APC-conjugated), anti-CD11a (PE-conjugated), anti-CD49d (PE-conjugated), anti-CD18 (FITC-conjugated), anti-IL-17 (PE-conjugated), and anti-Foxp3 (FITC-conjugated) were purchased from BD Biosciences. After cells were labeled with the appropriate antibodies for 30 min on ice and fixed in 1% paraformaldehyde in PBS, they were subjected to flow cytometry on a FACScalibur (BD Biosciences). Data were analyzed using the FlowJo software (Tree Star, Ashland, OR). Myeloid cells in bone marrow were identified as Gr-1$^{high}$ CD11b$^{+}$ and Gr-1$^{low}$ CD11b$^{+}$. Neutrophils in blood and spleen were identified as Gr-1$^{high}$ CD11b$^{+}$ cells and monocytes as Gr-1$^{low/-}$ CD11b$^{+}$ cells. T lymphocytes were identified as CD4$^{+}$ or CD8$^{+}$ cells and B lymphocytes as B220$^{+}$ cells. Th-17 cells were detected by determining the intracellular production of IL-17 in CD4$^{+}$ cells. Lymphocytes were isolated from mesenteric lymph nodes, activated with 50 ng/ml phorbol 12-myristate 13-acetate and 500 ng/ml ionomycin for 2 h and incubated with BD GolgiPlug (BD Biosciences) for 2 h. Cells were then stained with anti-CD4 PerCP-conjugated antibody on ice for 30 min, fixed, and permeabilized using the BD Cytofix/Cytoperm kit (BD Biosciences), and stained with IL-17 PE-conjugated and Foxp3 FITC-conjugated antibodies. Th-17 cells were identified as CD4$^{+}$ IL-17$^{+}$ Foxp3$^{-}$ cells.

*BrdU Labeling*—For bromodeoxyuridine (BrdU) labeling, mice were injected intraperitoneally once with 100 $\mu$l of a 10 mg/ml BrdU solution (BD Biosciences) and analyzed 48 h later. BrdU-positive cells were detected using a FITC-BrdU Flow kit (BD Biosciences) by flow cytometry.

*Corticosterone Quantification*—Serum levels of corticosterone were determined by ELISA (AssayPro, St. Charles, MO).

*Cytokine Quantification*—Serum levels of cytokines IL-12, TNF, IFN-g, monocyte chemoattractant protein (MCP)-1, IL-10, and IL-6 were determined using the BD Cytometric Bead Array (CBA, BD Biosciences). Serum IL-17 was detected

by ELISA (R&D Systems, Minneapolis, MN). Serum granulocyte-colony stimulating factor (G-CSF) was detected using the mouse cytokine/chemokine LINCOplex kit from Millipore (St. Charles, MO). IL-23 expression was studied by determining the levels of the *Il23a* subunit mRNA by real-time-quantitative PCR (RT-qPCR) as described below.

*s-CD62L in Serum*—The concentration of shed, soluble CD62L (s-CD62L) in serum from *Sgpl1*$^{+/+}$ and *Sgpl1*$^{-/-}$ mice was determined by ELISA (R&D Systems).

*Chemotaxis Assay*—The response of neutrophils toward formyl-methionyl-leucyl-phenylalanine (fMLP) was studied using 6.5 mm Transwell inserts with a 5-$\mu$m pore size (Corning, Cambridge, MA). A splenocyte suspension in RPMI 1640 plus 0.4 mg/ml fatty acid-free (FAF)-BSA (Sigma-Aldrich) (medium + FAF-BSA) was added to each insert in a well containing 600 $\mu$l of a solution of 1 $\mu$M fMLP (SigmaAldrich) prepared in medium + FAF-BSA. Wells containing medium + FAF-BSA without fMLP were used as controls. After 3 h at 37 °C, cells in the bottom of the wells were harvested, counted, and analyzed by flow cytometry.

*Gene Expression*—For RT-qPCR, total RNA was purified from bone marrow neutrophils and from liver using TRIZOL (Invitrogen). The mRNA expression levels of mouse *Tnf* (Mm00443258_m1), *Vcam-1* (Mm00449197_m1), *Saa1* (Mm00656927_g1), *Saa3* (Mm00441203_m1), *Sell* (Mm00441291_m1), *Il23a* (Mm00518984_m1), *S1pr1* (Mm00514644_m1), *S1pr2* (Mm01177794), *S1pr3* (Mm00515669_m1), *S1pr4* (Mm00468695_s1), and *S1pr5* (Mm00474763_m1) genes were determined by RT-qPCR using Assay-on-Demand probes and primers (Applied Biosystems, Foster City, CA) on an ABI Prism 7700 Sequence Detection System (Applied Biosystems). Glyceraldehyde-3-phosphate dehydrogenase (Mm99999915_g1) mRNA level was used as an internal control. For microarray analysis, RNA purified from *Sgpl1*$^{+/+}$ and *Sgpl1*$^{-/-}$ livers was prepared and analyzed on Affymetrix GeneChip Mouse Genome 430 2.0 arrays as described (29). The National Center for Biotechnology Information Gene Expression Omnibus accession number for the microarray data is GSE18745. Genes that belong to the Gene Ontology (GO) category "acute inflammation" were compared between *Sgpl1*$^{+/+}$ and *Sgpl1*$^{-/-}$ mRNA samples using a heat map generated using the Partek Genomic Suite 6.5 software (Partek Inc., St. Louis, MO).

*Lipid Analysis of Serum*—Sphingolipids in serum were measured by high-performance liquid chromatography-tandem mass spectrometry (HPLC-MS/MS) by the Lipidomics Core at the Medical University of South Carolina on a Thermo Finnigan (Waltham, MA) TSQ 7000 triple quadrupole mass spectrometer, operating in a multiple reaction monitoring-positive ionization mode as described (32).

*Statistical Analysis*—Statistical significance was determined using the Mann-Whitney or Student's *t* test. In all cases, values of $p < 0.05$ were considered statistically significant.

## RESULTS

*Profound Neutrophilia in Sgpl1*$^{-/-}$ *Mice*—*Sgpl1*$^{-/-}$ mice generally die soon after weaning (26, 28, 29), necessitating studies on young mice, at P18 unless otherwise indicated. The *Sgpl1*$^{-/-}$ mice were severely lymphopenic, with deficiencies of both T (CD4$^+$, CD8$^+$) cells and B (B220$^+$) cells in blood (supplemental Fig. S1, *A* and *C*). Low numbers of T and B cells were also apparent in the spleen of the *Sgpl1*$^{-/-}$ mice (supplemental Fig. S1, *B* and *D*). The lymphocyte deficiency in the *Sgpl1*$^{-/-}$ mice has been attributed to a number of possible sources, including a block in the egress of recirculating lymphocytes from secondary lymphoid organs and to defects in the development of T cells and B cells (27). In contrast to the severe lymphopenia, blood levels of neutrophils, and monocytes were highly elevated in the *Sgpl1*$^{-/-}$ mice (Fig. 1*A*) (26). *Sgpl1*$^{+/-}$ mice had normal blood cell counts indicating that both *Sgpl1* alleles must to be deleted to produce this immune phenotype (supplemental Fig. S2*A*).

We next determined the numbers and percentages of neutrophils and monocytes in the spleen and their precursors in the bone marrow. Compared with the WT mice, the percentages of splenic neutrophils and monocytes were dramatically elevated in *Sgpl1*$^{-/-}$ compared with WT mice (Fig. 1*C*). The total numbers of neutrophils and monocytes in spleen, when normalized by body weight, were also significantly increased in the *Sgpl1*$^{-/-}$ mice compared with WT mice (Fig. 1*D*). We enumerated myeloid cells, the precursors of neutrophils and monocytes, in bone marrow and found a substantial increase of both immature and mature myeloid cells in the *Sgpl1*$^{-/-}$ mice when expressed as either percentage of total cells or absolute cell numbers normalized by body weight (Fig. 1, *E* and *F*). The ratio of immature to mature myeloid cells was similar between *Sgpl1*$^{-/-}$ and WT mice suggesting differentiation of neutrophil precursors in the bone marrow of *Sgpl1*$^{-/-}$ mice was normal.

To establish whether increased granulopoiesis was responsible for the elevated neutrophil numbers in *Sgpl1*$^{-/-}$ mice, we labeled proliferating precursor cells in bone marrow by BrdU incorporation and determined the appearance of BrdU$^+$ neutrophils in blood after 48 h. The numbers of BrdU$^+$ neutrophils generated in *Sgpl1*$^{-/-}$ mice were significantly higher than in WT mice (Fig. 1*B*). These data indicate that increased granulopoiesis was occurring in the *Sgpl1*$^{-/-}$ mice.

We also determined the circulating ceramide, sphingosine, and S1P levels at P6 and P18 by HPLC-MS/MS analysis (supplemental Fig. S3). Both ceramide and S1P levels were substantially elevated at P6 and P18 in the *Sgpl1*$^{-/-}$ mice compared with WT mice. With increasing age, ceramide and S1P levels increased in the *Sgpl1*$^{-/-}$ mice. Sphingosine remained at similar low levels at both ages tested. *Sgpl1*$^{+/-}$ mice had serum sphingolipid levels similar to WT mice (supplemental Fig. S2*B*).

To rule out stress-induced changes on peripheral lymphocytes and neutrophils, we measured circulating corticosterone levels and found that there was no significant difference between the values of *Sgpl1*$^{-/-}$ and WT mice (supplemental Fig. S4).

*Inflammation in Sgpl1*$^{-/-}$ *Mice*—Neutrophilia can be associated with inflammation. Microarray analysis of P18 liver mRNA using Affymetrix mouse genome GeneChips revealed that the GO category of "acute inflammation" was signifi-

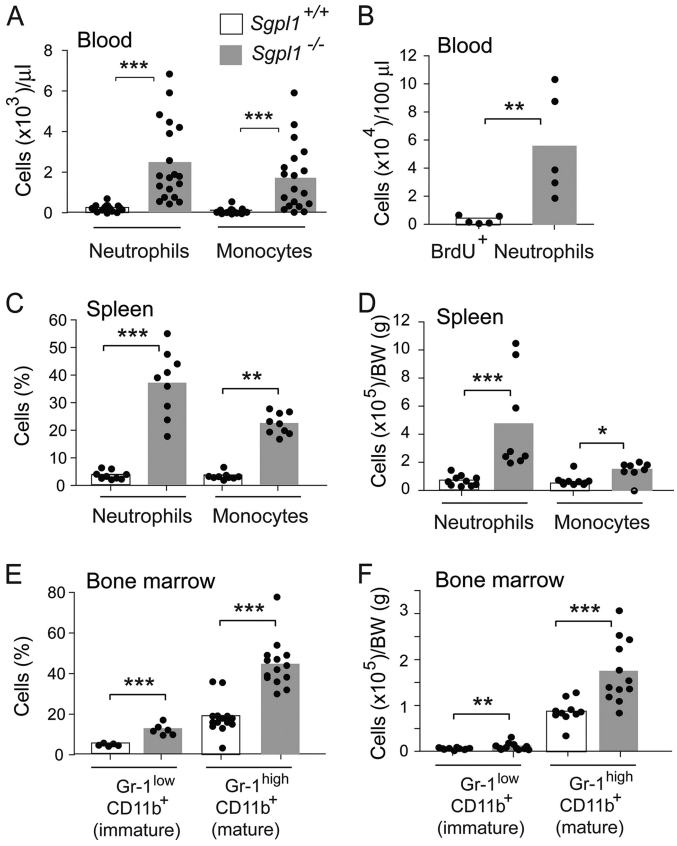


FIGURE 1. **Numbers of neutrophils and monocytes are increased in *Sgpl1*$^{-/-}$ mice.** *A*, numbers of neutrophils and monocytes in the blood of *Sgpl1*$^{+/+}$ and *Sgpl1*$^{-/-}$ mice. Cells were stained with anti-Gr-1 and anti-CD11b antibodies and analyzed by flow cytometry. Neutrophils were identified as Gr-1$^{high}$ CD11b$^{+}$ and monocytes as Gr-1$^{low/-}$ CD11b$^{+}$. Results are shown as the number of cells per μl of blood. The *bars* represent mean values, and the *closed circles* are individual mice. *B*, increased granulopoiesis in *Sgpl1*$^{-/-}$ mice. *Sgpl1*$^{+/+}$ and *Sgpl1*$^{-/-}$ mice were pulsed with BrdU, and neutrophils from peripheral blood were analyzed by flow cytometry using anti-Gr-1 and anti-CD11b antibodies in combination with BrdU detection. Results are shown as absolute numbers of BrdU$^{+}$ Gr-1$^{+}$ CD11b$^{+}$ neutrophils per 100 μl of blood. The *bars* represent mean values and the *closed circles* are individual mice. *C* and *D*, flow cytometry analysis of neutrophils and monocytes in spleen from *Sgpl1*$^{+/+}$ and *Sgpl1*$^{-/-}$ mice. Neutrophils and monocytes were identified as in *A*. Results are shown as the percentage of cells analyzed (*C*) and absolute numbers normalized by body weight (*D*). The *bars* represent mean values, and the *closed circles* are individual mice. *E* and *F*, flow cytometry analysis of myeloid progenitor cells in bone marrow from *Sgpl1*$^{+/+}$ and *Sgpl1*$^{-/-}$ mice. Myeloid progenitor cells were identified as Gr-1$^{low}$ CD11b$^{+}$ (immature) and Gr-1$^{high}$ CD11b$^{+}$(mature). Results are shown as the percentage of cells analyzed (*E*) and absolute numbers normalized by body weight (*F*). The *bars* represent mean values, and the *closed circles* are individual mice. *Sgpl1*$^{+/+}$ mice (*open bars*), *Sgpl1*$^{-/-}$ mice (*gray bars*). All mice were analyzed at P18. *, $p < 0.05$; **, $p < 0.01$; ***, $p < 0.005$. *ns*, not significant.

cantly different between *Sgpl1*$^{-/-}$ and WT mice ($p < 0.001$). Acute-phase reactants, serum amyloids (*Saa1–4*), orosomucoids (*Orm1–3*), and LPS binding protein (*Lbp*) were highly elevated in the livers of the *Sgpl1*$^{-/-}$ mice compared with those of WT mice, indicative of an acute inflammatory process (Fig. 2*A*).

We next determined the progression of inflammatory changes in *Sgpl1*$^{-/-}$ mice by examining the mRNA expression of some genes related to inflammation in liver at P6 and P18. An increase in *Tnf*, *Saa1*, and *Saa3* was detected by RT-qPCR at both ages in the *Sgpl1*$^{-/-}$ livers compared with those of WT mice (Fig. 2*B*). We also detected an increase in the expression level of the endothelial adhesion molecule *Vcam-1* in the P18 *Sgpl1*$^{-/-}$ livers when compared with controls (Fig. 2*B*). Vcam-1 is elevated during the endothelium response to inflammatory stimuli (33). Together, these results indicate the presence of a pro-inflammatory process in the liver of *Sgpl1*$^{-/-}$ mice that intensifies with age.

In the serum of *Sgpl1*$^{-/-}$ mice, we detected a significant increase in the levels of the pro-inflammatory cytokines TNF, IFN-γ, MCP-1, and IL-6 compared with levels observed in WT mice (Fig. 2*C*), demonstrating that the inflammation was systemic. *Sgpl1*$^{+/-}$ mice did not display any elevated serum cytokine levels (supplemental Fig. S2*C*). Injection of *Sgpl1*$^{-/-}$ mice with a dose of LPS, which was not lethal to WT mice, caused their death by 8 h (supplemental Fig. S5*A*). Within 120 min after the LPS injection, the *Sgpl1*$^{-/-}$ mice expressed substantially higher levels of TNF, IL-6, and MCP-1 in serum compared with the WT mice injected with LPS (supplemental Fig. S5*B*). Serum ceramide, sphingosine, and S1P concentrations were not significantly elevated over the respective baseline values in either *Sgpl1*$^{-/-}$ or control mice after LPS treatment during the same time period (supplemental Fig. S5*C*).

The pro-inflammatory state of the *Sgpl1*$^{-/-}$ mice raised the possibility that stimulation of the innate immune system by opportunistic bacterial infection, perhaps as a result of their severe lymphocyte deficiency, might be inducing systemic inflammation. We found no histologic evidence for the presence of infection in the tissue of *Sgpl1*$^{-/-}$ mice compared with WT mice (supplemental Fig. S6). We therefore studied the effect of deleting the Toll-like receptor-4 (Tlr4) in *Sgpl1*$^{-/-}$ mice (Fig. 3). Tlr4 is a receptor that detects the LPS of Gram-negative bacterial cell walls, and triggers a cascade of events that activates the transcription of many pro-inflammatory genes involved in the innate immune response (34). If the inflammatory response in *Sgpl1*$^{-/-}$ mice was the result of a Gram-negative bacterial infection, the inflammation in the *Sgpl1*$^{-/-}$ *Tlr4*$^{-/-}$ double knock-out (DKO) mice should be suppressed relative to the *Sgpl1*$^{-/-}$ mice. We found that the *Sgpl1*$^{-/-}$ *Tlr4*$^{-/-}$ DKO and *Sgpl1*$^{-/-}$ mice had similarly depressed lymphocyte and elevated neutrophil blood counts (Fig. 3*A*) and similar elevations of pro-inflammatory cytokines in serum (Fig. 3*B*) and of mRNA levels for *Tnf* and *Vcam-1* in liver (Fig. 3*C*). Whereas the *Sgpl1*$^{-/-}$ mice were hypersensitive to LPS, dying by 8 h after being challenged with a nonlethal dose of LPS, the *Sgpl1*$^{-/-}$ *Tlr4*$^{-/-}$ DKO mice were resistant (supplemental Fig. S5*A*). These results indicate that the pro-inflammatory condition of the *Sgpl1*$^{-/-}$ mice was unlikely to be the result of an activation of the innate immune system by an opportunistic Gram-negative bacterial infection.

*Impaired Neutrophil Migration into Sites of Inflammation in Sgpl1*$^{-/-}$ *Mice*—We next sought to determine if the neutrophilia was correlated with large numbers of neutrophils infiltrating into the liver of *Sgpl1*$^{-/-}$ mice, as would be expected based on the acute inflammation exhibited by this tissue (Fig. 2, *A* and *B*). Surprisingly, we found that the liver parenchyma in *Sgpl1*$^{-/-}$ mice appeared similar to *Sgpl1*$^{+/+}$

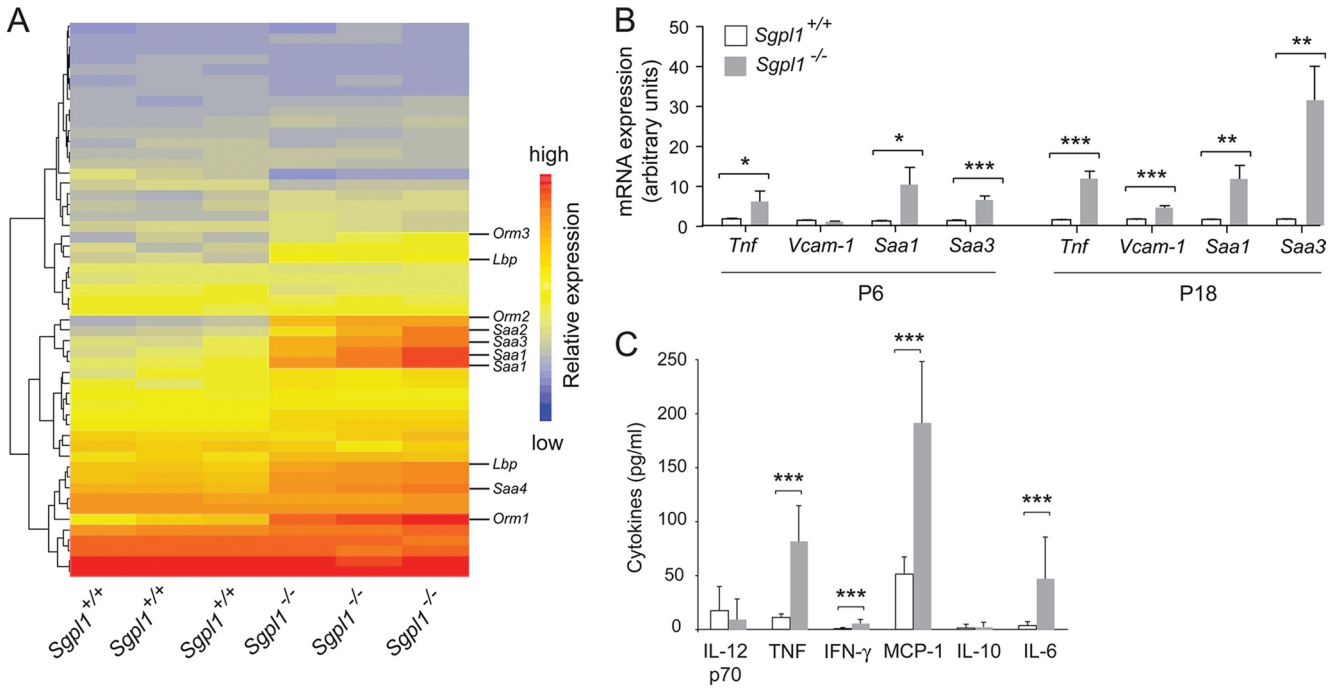


FIGURE 2. **Pro-inflammatory markers are elevated during development in *Sgpl1*$^{-/-}$ mice.** *A*, affymetrix microarray gene expression analysis was performed with liver mRNA from p18 *Sgpl1*$^{+/+}$ and *Sgpl1*$^{-/-}$ mice ($n = 3$ per genotype). The raw signal values of the genes from the GO category "acute inflammatory response" were clustered to produce a heat map. *Red* color corresponds to higher expression relative to *blue*. Probe sets corresponding to acute phase reactants, *Orm1–3*, *Saa1–4*, and *Lbp*, are indicated. *B*, expression of mRNA for genes related to the inflammatory response in the liver of *Sgpl1*$^{+/+}$ and *Sgpl1*$^{-/-}$ mice at P6 and at P18. RT-qPCR was performed on liver mRNA from *Sgpl1*$^{+/+}$ and *Sgpl1*$^{-/-}$ mice. Data are shown as mean values ± S.D. $n = 6$ mice per genotype for P6 and $n = 7$ for P18. *C*, concentrations of pro-inflammatory cytokines in the serum of *Sgpl1*$^{+/+}$ (*open bars*) and *Sgpl1*$^{-/-}$ (*gray bars*) mice. Concentration of serum pro-inflammatory cytokines determined using the BD CBA Array. Data are shown as mean values ± S.D. $n = 8$ for *Sgpl1*$^{+/+}$, $n = 12$ for *Sgpl1*$^{-/-}$ mice. *Sgpl1*$^{+/+}$ mice (*open bars*), *Sgpl1*$^{-/-}$ mice (*gray bars*). *, $p < 0.05$; **, $p < 0.01$; ***, $p < 0.005$.

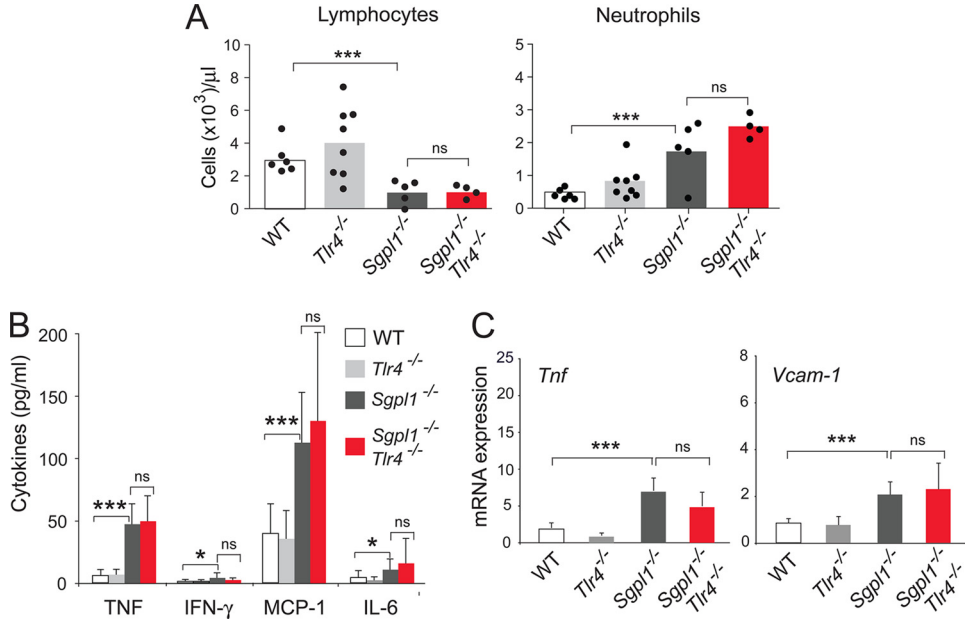


FIGURE 3. **Tlr4 deletion does not affect neutrophil levels in blood or pro-inflammatory markers in *Sgpl1*$^{-/-}$ mice.** Lymphocyte and neutrophil blood numbers, pro-inflammatory cytokines in serum, and inflammatory-related markers in liver in WT (*open bars*), *Sgpl1*$^{-/-}$ (*light gray bars*), *Tlr4*$^{-/-}$ (*dark gray bars*), and *Sgpl1*$^{-/-}$ *Tlr4*$^{-/-}$ DKO (*red bars*) mice. *A*, blood lymphocyte and neutrophil counts were determined by the Department of Laboratory Medicine at the NIH using an automated blood cell analyzer. Results are shown as number of cells per μl of blood. The *bars* represent mean values, and the *closed circles* are individual mice. *B*, concentration of pro-inflammatory cytokines in serum determined using the BD CBA Array. Data are shown as mean values ± S.D., $n = 9–17$ mice per genotype. *C*, *Tnf* and *Vcam-1* mRNA expression in liver determined using RT-qPCR. Data are shown as mean values ± S.D., $n = 4$ mice per genotype, all mice were analyzed at P18. *, $p < 0.05$; ***, $p < 0.005$. *ns*, not significant.

mice and did not exhibit extensive neutrophil infiltration (Fig. 4, *A* and *B*); however, we did observe abnormally high accumulations of neutrophils that appeared to be confined at the hepatic sinusoids in *Sgpl1*$^{-/-}$ mice compared with *Sgpl1*$^{+/+}$ mice (Fig. 4, *C* and *D*). These results suggested a possible impairment of neutrophil recruitment from the blood into the

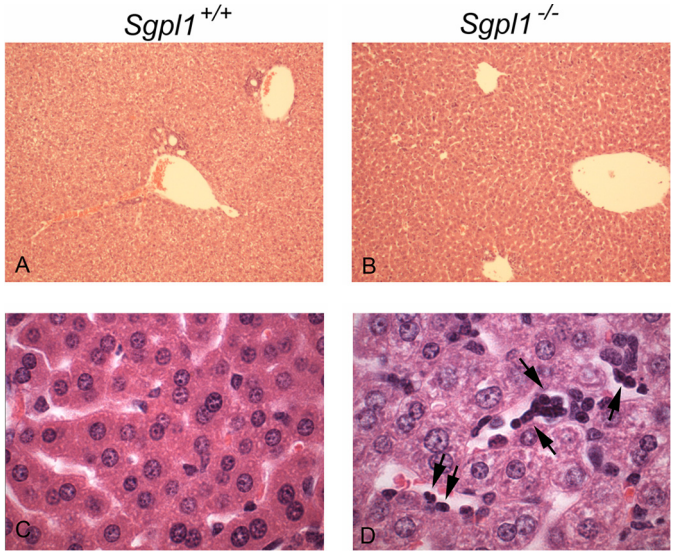


FIGURE 4. **Neutrophils are confined to the sinusoids in the liver of *Sgpl1*$^{-/-}$ mice.** Paraffin sections from liver from *Sgpl1*$^{+/+}$ (*A*, *C*) and *Sgpl1*$^{-/-}$ (*B*, *D*) mice were stained with H&E and examined on a Leica DMLB microscope. All mice were analyzed at P18. *A* and *B*, ×10 magnification. *C* and *D*, ×100 magnification. *Arrows* point to leukocytes in the hepatic sinusoids.

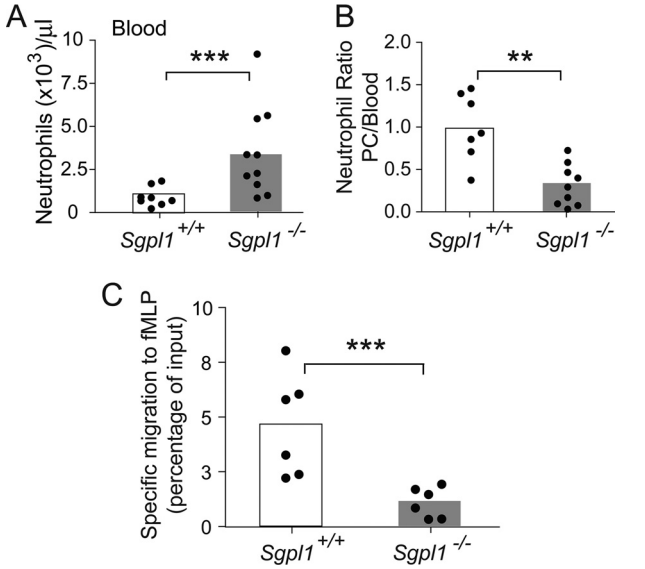


FIGURE 5. **Neutrophil migration is impaired in *Sgpl1*$^{-/-}$ mice.** *A* and *B*, *Sgpl1*$^{+/+}$ and *Sgpl1*$^{-/-}$ mice were injected intraperitoneal with thioglycollate. After 4 h, blood neutrophils and peritoneal neutrophils in the lavage were analyzed by flow cytometry. *A*, neutrophil blood counts after thioglycollate treatment. *B*, efficiency of neutrophil recruitment into the peritoneal cavity (*PC*) was determined by dividing the concentration of neutrophils obtained in the peritoneal lavage by the concentration of neutrophils in blood after thioglycollate treatment. Results are shown as neutrophil counts per μl of blood (*A*) and ratio of neutrophil counts in the PC/neutrophil counts in blood. *C*, deletion of *Sgpl1* alters the migration capacity of neutrophils toward fMLP. Total splenocytes from *Sgpl1*$^{+/+}$ and *Sgpl1*$^{-/-}$ mice were added to a Transwell insert and allowed to respond to 1 μM fMLP in the lower well. Percentages of the input that were found in the lower well after a 3-h incubation were plotted for neutrophils. *Bars* represent averages, and *circles* individual mice. $n = 6$ in three independent experiments. The *bars* represent mean values, and the *closed circles* are individual mice. *Sgpl1*$^{+/+}$ mice (*open bars*), *Sgpl1*$^{-/-}$ mice (*gray bars*). All mice were analyzed at P18. **, $p < 0.01$; ***, $p < 0.005$.

inflamed tissue in the *Sgpl1*$^{-/-}$ mice. A survey of other *Sgpl1*$^{-/-}$ tissues showed that they were spared from substantial neutrophil infiltration (supplemental Fig. S6, *C–L*). As reported previously (26), the *Spgl1*$^{-/-}$ lungs contained a slight increase in macrophages within alveoli (supplemental Fig. S6, *A* and *B*).

To establish whether *Sgpl1* deficiency altered the ability of neutrophils to migrate to sites of inflammation, we injected mice intraperitoneal with thioglycollate and examined the influx of neutrophils into the peritoneal cavity after 4 h. We calculated the number of neutrophils recruited into the peritoneum relative to the available neutrophils in the blood (Fig. 5, *A* and *B*) and found that *Sgpl1*$^{-/-}$ mice had a significantly lower efficiency of neutrophil recruitment into thioglycollate-treated peritoneum than did the WT mice (Fig. 5*B*).

We tested the ability of neutrophils from *Sgpl1*$^{-/-}$ mice to migrate to a chemotaxic stimulus. As shown in Fig. 5*C*, neutrophils from *Sgpl1*$^{-/-}$ mice were significantly impaired relative to WT neutrophils in their ability to migrate toward fMLP peptide.

*Abnormal Adhesion Molecule Expression on Neutrophils of Sgpl1*$^{-/-}$ *Mice*—Because mice deficient in some adhesion molecules show neutrophilia and/or impaired recruitment to sites of inflammation (35–46) similar to that observed for Sgpl1$^{-/-}$ mice, we next determined the expression profile of adhesion molecules on blood neutrophils in *Sgpl1*$^{+/+}$ (WT) and *Sgpl1*$^{-/-}$ mice. *Sgpl1*$^{-/-}$ blood neutrophils expressed substantially lower levels of CD62L (L-selectin), than neutrophils from WT blood (Fig. 6, *A* and *F*). In addition, the surface expression of CD11b (integrin αM or Mac-1), CD11a (integrin αL), CD18 (integrin β2), and CD49d (integrin α2) on blood neutrophils was all significantly decreased in *Sgpl1*$^{-/-}$ mice compared with WT mice (Fig. 6, *B–E* and *G–J*).

The lower levels of CD62L on the *Sgpl1*$^{-/-}$ neutrophils did not appear to be the result of enhanced surface shedding of this molecule, because the serum levels of soluble CD62L were similar in *Sgpl1*$^{-/-}$ and *Sgpl1*$^{+/+}$ mice (supplemental Fig. S7*A*). Instead, the lower expression levels correlated with a significantly lower expression of CD62L (*Sell*) mRNA in *Sgpl1*$^{-/-}$ compared with *Sgpl1*$^{+/+}$ mice (supplemental Fig. S7*B*).

*Neutrophilia and Inflammation Are Conferred by the Sgpl1*$^{-/-}$ *Hematopoietic System*—To determine if the neutrophilia and inflammation phenotype could be conferred by the *Sgpl1*$^{-/-}$ hematopoietic system, we established *Sgpl1*$^{-/-}$ chimeras by transplanting bone marrow cells from *Sgpl1*$^{-/-}$ donors into WT *Rag2*$^{-/-}$ recipients (*Sgpl1*$^{-/-}$ → *Rag2*$^{-/-}$). *Rag2*$^{-/-}$ mice lack mature T and B cells, which can be restored by transplantation with recipient bone marrow cells. Compared with control chimeras that received *Sgpl1*$^{+/+}$ bone marrow cells (*Sgpl1*$^{+/+}$ → *Rag2*$^{-/-}$), the *Sgpl1*$^{-/-}$ chimeras showed higher neutrophil levels and lower T-cell numbers in blood, higher TNF and IL-6 levels in serum, and higher *Tnf* and *Vcam-1* mRNA in liver (Fig. 7, *A–C*). Furthermore, blood neutrophils from the *Sgpl1*$^{-/-}$ chimeras expressed lower surface levels of CD62L compared with neutrophils from the control chimeras (Fig. 7*D*). The circulating S1P levels, but not the ceramide or sphingosine, were significantly elevated in the *Sgpl1*$^{-/-}$ chimeras compared with the *Sgpl1*$^{+/+}$ chimeras (Fig. 7*E*).

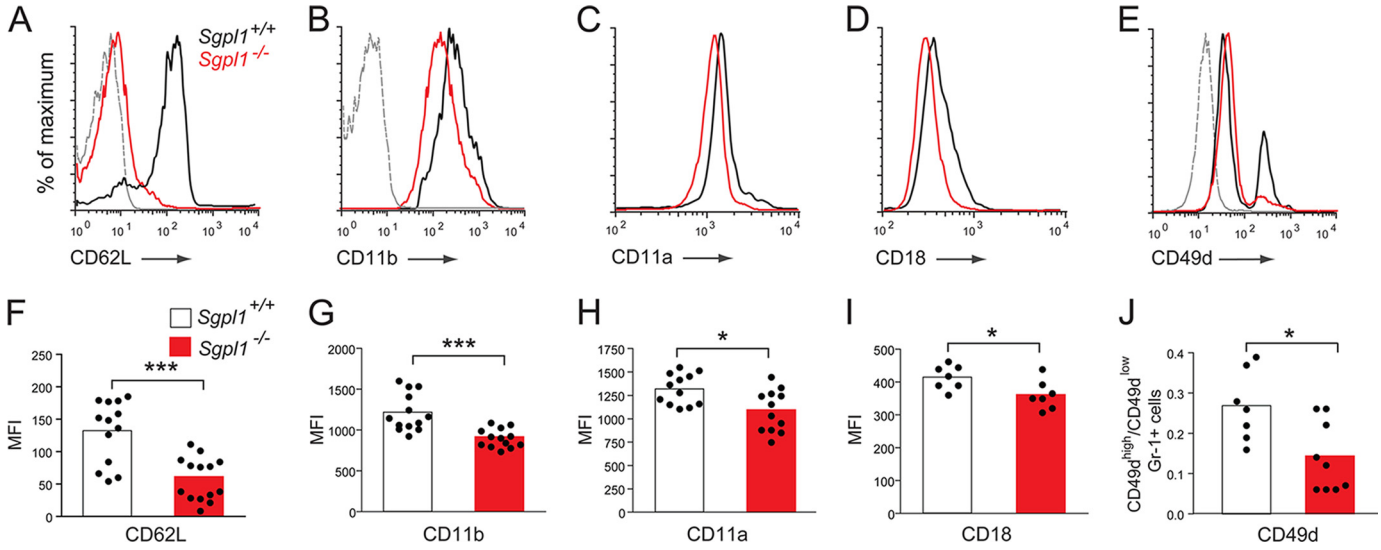


FIGURE 6. **Expression of adhesion molecules is decreased on neutrophils from *Sgpl1*$^{-/-}$ mice.** Blood neutrophils were analyzed by flow cytometry for the expression of CD62L (*A*, *F*), CD11b (*B*, *G*), CD11a (*C*, *H*), CD18 (*D*, *I*), and CD49d (*E*, *J*). Results are shown as histograms (*A–E*), mean fluorescence intensity (MFI) (*F–I*), and the ratio of CD49d$^{high}$/CD49d$^{low}$ Gr-1$^{+}$ cells (*J*) from *Sgpl1*$^{+/+}$ and *Sgpl1*$^{-/-}$ mice. In *A*, *B*, and *E*, isotype control staining is shown as a *dotted line*. In *F–J*, the *bars* represent mean values, and the *closed circles* are individual mice. *Sgpl1*$^{+/+}$ mice (*black lines* and *open bars*), *Sgpl1*$^{-/-}$ mice (*red lines* and *red bars*). All mice were analyzed at P18. *, $p < 0.05$; ***, $p < 0.005$.

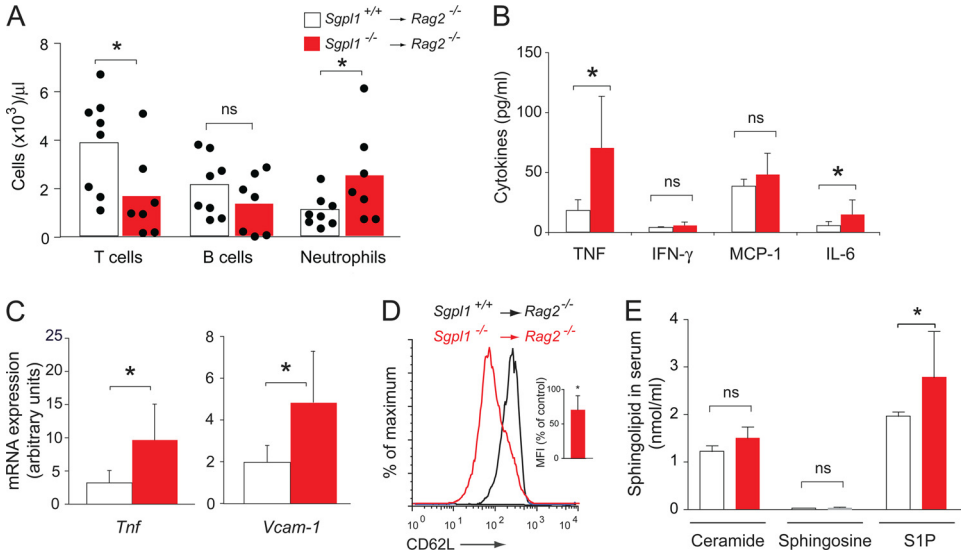


FIGURE 7. **Neutrophilia and inflammation are transferred by *Sgpl1*$^{-/-}$ bone marrow-derived hematopoietic cells.** Total bone marrow cells from p18 *Sgpl1*$^{+/+}$ and *Sgpl1*$^{-/-}$ mice were injected i.v. into lethally irradiated adult *Rag2*$^{-/-}$ mice to generate control *Sgpl1*$^{+/+}$ → *Rag2*$^{-/-}$ and *Sgpl1*$^{-/-}$ → *Rag2*$^{-/-}$. Transplanted mice were analyzed 8 weeks after the procedure. *A*, blood cell counts determined by flow cytometry. Results are shown as number of cells per μl of blood. The *bars* represent mean values, and the *closed circles* are individual mice. *B*, concentration of pro-inflammatory cytokines in serum determined using the BD CBA Array. Data are shown as mean values ± S.D., $n = 9$ mice per genotype. *C*, *Tnf* and *Vcam-1* mRNA expression in liver determined using RT-qPCR. Data are shown as mean values ± S.D. for *Sgpl1*$^{+/+}$ → *Rag2*$^{-/-}$ mice ($n = 5$) and for *Sgpl1*$^{-/-}$ → *Rag2*$^{-/-}$ mice ($n = 6$). *D*, CD62L expression on the surface of blood neutrophils was analyzed by flow cytometry. Results are shown as a histogram. The inset shows the mean fluorescence intensity (MFI) for *Sgpl1*$^{-/-}$ → *Rag2*$^{-/-}$ ($n = 5$) neutrophils as percentage of control *Sgpl1*$^{+/+}$ → *Rag2*$^{-/-}$ ($n = 4$) neutrophil values. Data are shown as mean values ± S.D. *E*, sphingolipid concentration in serum analyzed by HPLC-MS/MS. Data are shown as mean values ± S.D., $n = 12$ mice per genotype. *Sgpl1*$^{+/+}$ → *Rag2*$^{-/-}$ (*open bars* and *black line*) and *Sgpl1*$^{-/-}$ → *Rag2*$^{-/-}$ (*red bars* and *red line*). *, $p < 0.05$. *ns*, not significant.

*S1P4 Receptor Contributes to Inflammatory Responses in Sgpl1*$^{-/-}$ *Mice*—We next determined whether the neutrophilia and the increase in pro-inflammatory markers in the Sgpl1$^{-/-}$ mice were mediated through S1P receptors. Neutrophils purified from Sgpl1$^{+/+}$ mice expressed *S1pr1* and *S1pr4* mRNA at higher levels compared with *S1pr2*, *S1pr3*, and *S1pr5* mRNA (supplemental Fig. S8). We therefore generated DKO mice for the *Sgpl1* gene together with *S1pr1* or with *S1pr4* genes (Fig. 8). Because the *S1pr1* deletion causes lethality during embryogenesis, we deleted *S1pr1* specifically in macrophages and granulocytes (Gr-*S1pr1*KO).

*Sgpl1*$^{-/-}$ Gr-S1pr1KO mice did not significantly differ from the single mutant *Sgpl1*$^{-/-}$ mice in blood levels of lymphocytes and neutrophils and in serum concentrations of pro-inflammatory cytokines (Fig. 8, *A* and *B*). In contrast, *Sgpl1*$^{-/-}$ *S1pr4*$^{-/-}$ mice had significantly lower blood neutrophil counts and serum pro-inflammatory cytokines than the single-mutant *Sgpl1*$^{-/-}$ mice, although both *Sgpl1*$^{-/-}$

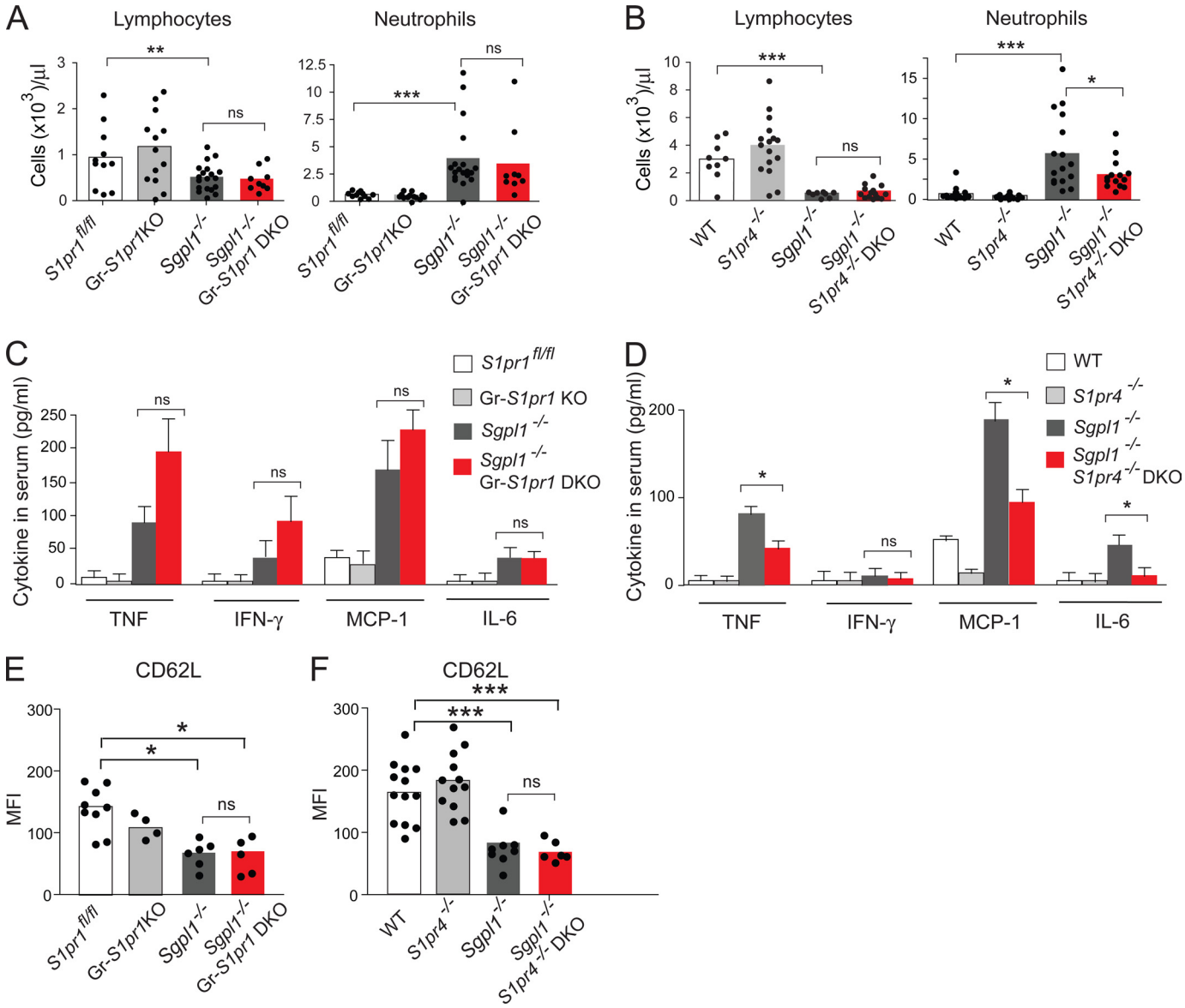


FIGURE 8. **S1pr4 deletion lowers blood neutrophil levels and inflammatory markers in *Sgpl1*$^{-/-}$ mice.** *S1Pr1*$^{fl/fl}$, Gr-*S1pr1*KO, *Sgpl1*$^{-/-}$, and *Sgpl1*$^{-/-}$ Gr-*S1pr1*KO DKO mice (*A*, *C*, *E*), and WT, *S1pr4*$^{-/-}$, *Sgpl1*$^{-/-}$, and *Sgpl1*$^{-/-}$ *S1pr4*$^{-/-}$ DKO mice (*B*, *D*, *F*) were analyzed for blood cell counts, pro-inflammatory cytokines, and CD62L expression on neutrophils. *A* and *B*, blood lymphocyte and neutrophil counts were determined by the Department of Laboratory Medicine at the NIH using an automated blood cell analyzer. Results are shown as number of cells per μl of blood. The *bars* represent mean values, and the *closed circles* are individual mice. Results are shown as number of cells per μl of blood. The *bars* represent mean values, and the *closed circles* are individual mice. *C* and *D*, concentration of pro-inflammatory cytokines in serum determined using the BD CBA Array. Data are shown as mean values ± S.D., $n = 5$. *E* and *F*, CD62L expression on the surface of blood neutrophils from DKO mice. *E*, expression levels of CD62L on *S1Pr1*$^{fl/fl}$, Gr-*S1pr1*KO, *Sgpl1*$^{-/-}$, and *Sgpl1*$^{-/-}$ Gr-*S1pr1* DKO neutrophils are shown as mean fluorescence intensity (MFI). *F*, expression levels of CD62L on WT, *S1pr4*$^{-/-}$, *Sgpl1*$^{-/-}$, and *Sgpl1*$^{-/-}$ *S1pr4*$^{-/-}$ DKO neutrophils are shown as the MFI. The *bars* represent mean values, and the *closed circles* are individual mice. All mice were analyzed at P18. *, $p < 0.05$; **, $p < 0.01$; ***, $p < 0.005$. *ns*, not significant.

*S1pr4*$^{-/-}$, and *Sgpl1*$^{-/-}$ mice were similarly lymphopenic (Fig. 8, *D* and *E*). The expression of CD62L on the *Sgpl1*$^{-/-}$ neutrophils was not normalized by either the deletion of *S1pr1* or *S1pr4*$^{-/-}$ (Fig. 8, *E* and *F*). The results indicate that the S1P4 receptor plays a role in the extent of pro-inflammatory responses caused by the S1P lyase deficiency. However, the S1P1 receptor, when specifically deleted in the granulocyte lineage, does not alter the phenotype.

*Homeostatic Regulation of Neutrophil Production Is Abnormal in Sgpl1*$^{-/-}$ *Mice*—Neutrophils normally traffic to tissues where they undergo apoptosis and are phagocytosed by macrophages and dendritic cells, down-regulating cytokine production and leading to increased granulocyte production. When transmigration of neutrophils to tissues is blocked, as is the case in mice deficient in leukocyte or endothelial adhesion molecules, IL-23 production by macrophages and dendritic cells increases, stimulating IL-17 generation by T cells. IL-17 in turn induces G-CSF production, leading to higher granulopoiesis in the bone marrow and elevated circulating neutrophils (Fig. 9*E*) (47, 48).

We next determined if this negative feedback loop for neutrophil homeostasis was disrupted in the *Sgpl1*$^{-/-}$ mice. An increase in IL-23 mRNA expression was found in *Sgpl1*$^{-/-}$ lung, liver, kidney, and small intestine compared with levels

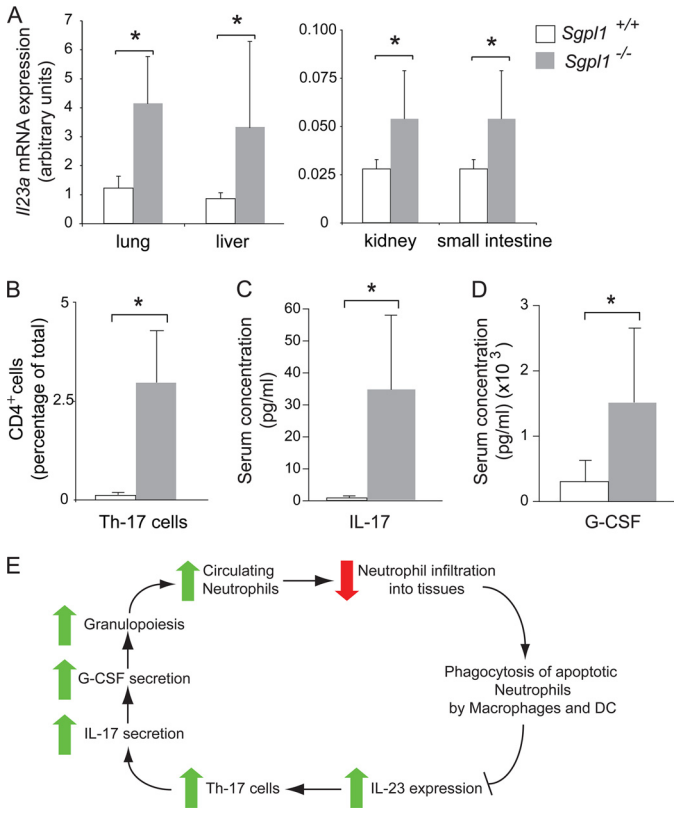


FIGURE 9. **Cytokine-controlled loop regulating neutrophil homeostasis is affected in *Sgpl1*$^{-/-}$ mice.** *A*, *Il23a* mRNA expression was determined in various tissues by RT-qPCR in *Sgpl1*$^{+/+}$ and *Sgpl1*$^{-/-}$ mice. Data are shown as mean values ± S.D. $n = 4–7$ mice for each genotype. *B*, CD4$^+$ T cells from mesenteric lymph nodes from *Sgpl1*$^{+/+}$ and *Sgpl1*$^{-/-}$ mice were stained for IL-17 expression and analyzed by flow cytometry. Data are shown as mean values ± S.D., $n = 6$. *C*, IL-17 was measured in the serum of *Sgpl1*$^{+/+}$ and *Sgpl1*$^{-/-}$ mice by ELISA. Data are shown as mean values ± S.D., $n = 5$. *D*, concentration of G-CSF in the serum of *Sgpl1*$^{+/+}$ and *Sgpl1*$^{-/-}$ mice determined using the mouse cytokine/chemokine LINCOplex kit. All mice were analyzed at P18. Data are shown as mean values ± S.D., $n = 7$. *E*, impact of the *Sgpl1* deletion on neutrophil homeostasis (*green* and *red arrows*) based on the model proposed by Klaus Ley and co-workers (47, 48). *Sgpl1* deletion impedes the migration of blood neutrophils into tissues. Tissue macrophages and dendritic cells respond to reduced phagocytosis of apoptotic neutrophils by increased Il-23 production leading to elevated 1L-17 and G-CSF synthesis. *Sgpl1*$^{+/+}$ (*open bars*) and *Sgpl1*$^{-/-}$ (*gray bars*). *, $p < 0.05$.

observed in *Sgpl1*$^{+/+}$ mice (Fig. 9*A*). To investigate IL-17 generation, we analyzed the presence of IL-17-producing Th-17 cells in mesenteric lymph nodes and found a significant increase in the percentage of IL-17$^+$ Foxp3$^-$ CD4$^+$ cells in the *Sgpl1*$^{-/-}$ mice compared with percentages observed in *Sgpl1*$^{+/+}$ mice (Fig. 9*B*). We also determined the serum concentration of IL-17 and found elevated levels of IL-17 in the serum of *Sgpl1*$^{-/-}$ mice compared with those in the serum of *Sgpl1*$^{+/+}$ mice (Fig. 9*C*). Finally, the G-CSF concentration in serum was significantly increased in the *Sgpl1*$^{-/-}$ mice compared with the G-CSF concentration in *Sgpl1*$^{+/+}$ mice (Fig. 9*D*).

## DISCUSSION

In the absence of S1P lyase, *Sgpl1*$^{-/-}$ mice lack the major degradation pathway for S1P and, as a result, express high levels of S1P in circulation and in tissues (26, 29). These mice show diverse phenotypic abnormalities including a shortened lifespan, abnormal lipid metabolism and severe immune system disturbances affecting both the adaptive and innate components.

As shown here, the *Sgpl1*$^{-/-}$ mice were deficient in B and T lymphocytes yet had high blood levels of neutrophils and monocytes along with elevated expression of pro-inflammatory cytokines. Surprisingly, their tissues were largely clear of infiltrating leukocytes.

Peripheral blood numbers of neutrophils are tightly regulated by a homeostatic feedback loop that controls granulopoiesis (Fig. 9*E*) (47, 48). Within the loop, IL-23 is expressed by tissue resident macrophages and dendritic cells to initiate a cytokine cascade that links IL-17 and G-CSF. First, IL-23 potently elevates IL-17 levels through increases in the numbers of IL-17-secreting T cells; then, IL-17 induces an increase in the levels of G-CSF, which promotes the proliferation of promyelocytes and the maturation of granulocytes in the bone marrow (47, 48). Normally, after release from the bone marrow, neutrophils move from blood to tissues, where they undergo apoptosis and are phagocytosed by macrophages and dendritic cells (47). This process of phagocytosis supplies a potent signal to macrophages and dendritic cells that suppresses IL-23 synthesis, closing the feedback loop.

We found that the *Sgpl1*$^{-/-}$ mice have disturbed neutrophil homeostasis. They have activation of the IL-23/IL-17/G-CSF cytokine axis leading to increased granulopoiesis. The increased neutrophil production in the bone marrow of the *Sgpl1*$^{-/-}$ mice did not appear to be the result of a bacterial infection, because their tissues appeared clear of infectious agents upon histologic examination, and because neutrophil numbers did not decrease when the LPS sensor *Tlr4* was deleted from the *Sgpl1*$^{-/-}$ mice. Instead, our results point to direct effects by the *Sgpl1* deficiency on neutrophil homostasis.

A key point in neutrophil homeostasis occurs with the transmigration of neutrophils across the endothelium and into tissues. When this step is blocked, as with mice with integrin and selectin deficiencies (35–46) or with humans with leukocyte adhesion deficiencies (49, 50), neutrophilia is a prominent feature. Adhesion molecules, both selectins and integrins, on neutrophils are essential for their interaction with the endothelium and entry into tissues (51). The increase in blood neutrophils is not a passive phenomenon in the adhesion molecule deficiencies, but rather is due to activation of the IL-23/IL-17/G-CSF cytokine axis. This axis is activated by the absence of suppressive signals due to the inability of neutrophils to transmigrate into tissues where they are phagocytosed by macrophages and dendritic cells (47, 48). As has been reported for several of the adhesion molecule knockout mice, the *Sgpl1*$^{-/-}$ mice exhibited reduced efficiency of the recruitment of neutrophils to sites of inflammation (35–46). The reduced expression of multiple adhesion molecules on the neutrophils in *Sgpl1*$^{-/-}$ mice is one mechanism to explain the reduced entry of blood neutrophils into tissues, thereby disrupting the homeostatic regulatory loop and activating the IL-23/IL-17/G-CSF pathway controlling granulopoiesis. The greatest adhesion molecule deficiency on the *Sgpl1*$^{-/-}$ neutrophils was found for CD62L, with smaller de-

creases in surface expression of CD11b, CD11a, CD18, and CD49d. Whereas a single deficiency of CD62L did not lead to neutrophilia in mice (37), compound deficiencies of CD62L with other adhesion molecules did result in elevated numbers of neutrophils in blood (42, 44, 45). The large decrease of surface CD62L expression on *Sgpl1*$^{-/-}$ neutrophils did not appear to be the result of enhanced shedding, which occurs during neutrophil activation, because the levels of soluble CD62L in serum were similar in *Sgpl1*$^{-/-}$ and *Sgpl1*$^{+/+}$ mice. Furthermore, levels of CD11b, a marker of neutrophil activation (52), were reduced on the *Sgpl1*$^{-/-}$ neutrophils. Instead, a transcriptional mechanism appeared to be responsible for the decreased expression of CD62L, because of significantly decreased levels of its mRNA in the *Sgpl1*$^{-/-}$ neutrophils.

The *Sgpl1*$^{-/-}$ neutrophils also displayed a reduced capacity *in vitro* to navigate toward a strong chemotaxic stimulus suggesting intrinsic defects in their migration response, which may also contribute to their reduced recruitment to imflamed tissues. Inhibition of chemotaxis by extracellular S1P have been reported previously for other cell types (53–55).

Heightened S1P levels in the *Sgpl1*$^{-/-}$ mice may also intersect at another point on the neutrophil homeostatic loop to enhance pro-inflammatory signaling. Acting through the S1P1 receptor on T cells, S1P has the same capacity as IL-23 to augment the number of Th-17 cells and the secretory activity of IL-17 by Th-17 cells (56). In the *Sgpl1*$^{-/-}$ mice, although the total numbers of T cells were reduced, the percentage of Th-17 cells was significantly elevated, demonstrating a specific enrichment of the Th-17 lineage. Th-17 cells are highly proinflammatory (57), and may contribute to the systemic inflammation observed in the *Sgpl1*$^{-/-}$ mice. IL-17 acts on many cell types to stimulate the production of pro-inflammatory cytokines, including TNF, IL-6, and MCP-1, which were all found to be elevated in the *Sgpl1*$^{-/-}$ mice. Sphingosine kinase and its product, S1P, have been shown to have pro-inflammatory effects by acting, in some cases, through cell-surface receptors (58–64). Also, intracellular S1P has recently been shown to act as a cofactor for the E3 ubiquitin-ligase TRAF2, which stimulates NF-κB activation (65).

The deletion of the S1P4 receptor in the *Sgpl1*$^{-/-}$ background caused a decrease in the pro-inflammatory responses, implying that signaling through the S1P4 receptor is contributing to this phenotype. Because S1P binds and activates the S1P4 receptor at concentrations that are substantially higher than those for the other S1P receptors (66), it is possible that the S1P4 receptor becomes engaged in the *Sgpl1*$^{-/-}$ mice due to high concentrations of S1P. The S1P4 receptor is widely expressed on the cells of the immune and hematopoietic systems (67, 68), suggesting several possible cellular sites of action (including on neutrophils, T cells, and macrophages). In T cells, the S1P4 receptor has been reported to regulate proliferation and cytokine secretion (69) and could potentially control the levels of cytokines expressed in the *Sgpl1*$^{-/-}$ mice. Excessive signaling through the S1P4 receptor does not seem to be the primary cause of the early demise of the *Sgpl1*$^{-/-}$ mice because the *Sgpl1*$^{-/-}$ *S1pr4*$^{-/-}$ DKO mice do not live longer than single mutant *Sgpl1*$^{-/-}$ mice (data not shown).

The partial normalization of the inflammatory phenotype in the *Sgpl1*$^{-/-}$ mice by the *S1pr4* deletion indicates that other receptor signaling pathways may be operating. The S1P1 receptor, when deleted within granulocytes and monocytes in the *Sgpl1*$^{-/-}$ mice, failed to significantly reduce the levels of pro-inflammatory markers observed in *Sgpl1*$^{-/-}$ mice; however, it is possible that the S1P1 receptor might function in other tissues or cells to regulate inflammatory pathways in the *Sgpl1*$^{-/-}$ mice. The S1P1 receptor has an important role in controlling endothelial barrier integrity (70), and its activation in endothelial cells in the *Sgpl1*$^{-/-}$ mice may impede neutrophil migration into tissues (Fig. 9*E*). The S1P1 receptor also activates the Stat3 pathway, which regulates the acute-phase response in liver and the generation of Th-17 cells, both features of the *Sgpl1*$^{-/-}$ mice (71–73).

Our results show that in the absence of S1P lyase activity pro-inflammatory responses are elevated while neutrophil migration into inflamed tissues is impaired, thereby disrupting homeostatic regulation of neutrophils. S1P lyase activity and the relevant S1P receptor signaling pathways represent new potential targets for manipulating neutrophil levels, their function, and inflammation.

*Acknowledgment—We thank Catherine Theisen for expert assistance.*

## REFERENCES


1. Rosen, H., and Goetzl, E. J. (2005) *Nat. Rev. Immunol.* **5,** 560–570
2. El Alwani, M., Wu, B. X., Obeid, L. M., and Hannun, Y. A. (2006) *Pharmacol. Ther.* **112,** 171–183
3. Kono, M., Allende, M. L., and Proia, R. L. (2008) *Biochim. Biophys. Acta* **1781,** 435–441
4. Rivera, J., Proia, R. L., and Olivera, A. (2008) *Nat. Rev. Immunol.* **8,** 753–763
5. Kim, R. H., Takabe, K., Milstien, S., and Spiegel, S. (2009) *Biochim. Biophys. Acta* **1791,** 692–696
6. Hannun, Y. A., and Obeid, L. M. (2008) *Nat. Rev. Mol. Cell Biol.* **9,** 139–150
7. Fyrst, H., and Saba, J. D. (2010) *Nat. Chem. Biol.* **6,** 489–497
8. Skoura, A., and Hla, T. (2009) *J. Lipid Res.* **50,** Suppl., S293–S298
9. Hla, T., Venkataraman, K., and Michaud, J. (2008) *Biochim. Biophys. Acta* **1781,** 477–482
10. Hänel, P., Andréani, P., and Gräler, M. H. (2007) *FASEB J.* **21,** 1202–1209
11. Ito, K., Anada, Y., Tani, M., Ikeda, M., Sano, T., Kihara, A., and Igarashi, Y. (2007) *Biochem. Biophys. Res. Commun.* **357,** 212–217
12. Pappu, R., Schwab, S. R., Cornelissen, I., Pereira, J. P., Regard, J. B., Xu, Y., Camerer, E., Zheng, Y. W., Huang, Y., Cyster, J. G., and Coughlin, S. R. (2007) *Science* **316,** 295–298
13. Yatomi, Y., Ohmori, T., Rile, G., Kazama, F., Okamoto, H., Sano, T., Satoh, K., Kume, S., Tigyi, G., Igarashi, Y., and Ozaki, Y. (2000) *Blood* **96,** 3431–3438
14. Jolly, P. S., Bektas, M., Watterson, K. R., Sankala, H., Payne, S. G., Milstien, S., and Spiegel, S. (2005) *Blood* **105,** 4736–4742
15. Venkataraman, K., Thangada, S., Michaud, J., Oo, M. L., Ai, Y., Lee, Y. M., Wu, M., Parikh, N. S., Khan, F., Proia, R. L., and Hla, T. (2006) *Biochem. J.* **397,** 461–471
16. Venkataraman, K., Lee, Y. M., Michaud, J., Thangada, S., Ai, Y., Bonkovsky, H. L., Parikh, N. S., Habrukowich, C., and Hla, T. (2008) *Circ. Res.* **102,** 669–676
17. Allende, M. L., Dreier, J. L., Mandala, S., and Proia, R. L. (2004) *J. Biol. Chem.* **279,** 15396–15401

18. Matloubian, M., Lo, C. G., Cinamon, G., Lesneski, M. J., Xu, Y., Brinkmann, V., Allende, M. L., Proia, R. L., and Cyster, J. G. (2004) *Nature* **427,** 355–360
19. Kabashima, K., Haynes, N. M., Xu, Y., Nutt, S. L., Allende, M. L., Proia, R. L., and Cyster, J. G. (2006) *J. Exp. Med.* **203,** 2683–2690
20. Walzer, T., Chiossone, L., Chaix, J., Calver, A., Carozzo, C., Garrigue-Antar, L., Jacques, Y., Baratin, M., Tomasello, E., and Vivier, E. (2007) *Nat. Immunol.* **8,** 1337–1344
21. Allende, M. L., Zhou, D., Kalkofen, D. N., Benhamed, S., Tuymetova, G., Borowski, C., Bendelac, A., and Proia, R. L. (2008) *FASEB J.* **22,** 307–315
22. Pereira, J. P., Xu, Y., and Cyster, J. G. (2010) *PLoS One* **5,** e9277
23. Allende, M. L., Tuymetova, G., Lee, B. G., Bonifacino, E., Wu, Y. P., and Proia, R. L. (2010) *J. Exp. Med.* **207,** 1113–1124
24. Schwab, S. R., Pereira, J. P., Matloubian, M., Xu, Y., Huang, Y., and Cyster, J. G. (2005) *Science* **309,** 1735–1739
25. Zachariah, M. A., and Cyster, J. G. (2010) *Science* **328,** 1129–1135
26. Vogel, P., Donoviel, M. S., Read, R., Hansen, G. M., Hazlewood, J., Anderson, S. J., Sun, W., Swaffield, J., and Oravecz, T. (2009) *PLoS One* **4,** e4112
27. Weber, C., Krueger, A., Münk, A., Bode, C., Van Veldhoven, P. P., and Gräler, M. H. (2009) *J. Immunol.* **183,** 4292–4301
28. Schmahl, J., Raymond, C. S., and Soriano, P. (2007) *Nat. Genet.* **39,** 52–60
29. Bektas, M., Allende, M. L., Lee, B. G., Chen, W., Amar, M. J., Remaley, A. T., Saba, J. D., and Proia, R. L. (2010) *J. Biol. Chem.* **285,** 10880–10889
30. Allende, M. L., Yamashita, T., and Proia, R. L. (2003) *Blood* **102,** 3665–3667
31. Clausen, B. E., Burkhardt, C., Reith, W., Renkawitz, R., and Förster, I. (1999) *Transgenic Res.* **8,** 265–277
32. Bielawski, J., Szulc, Z. M., Hannun, Y. A., and Bielawska, A. (2006) *Methods* **39,** 82–91
33. Barreiro, O., Martín, P., González-Amaro, R., and Sánchez-Madrid, F. (2010) *Cardiovasc. Res.* **86,** 174–182
34. Beutler, B. A. (2009) *Blood* **113,** 1399–1407
35. Wilson, R. W., Ballantyne, C. M., Smith, C. W., Montgomery, C., Bradley, A., O'Brien, W. E., and Beaudet, A. L. (1993) *J. Immunol.* **151,** 1571–1578
36. Mayadas, T. N., Johnson, R. C., Rayburn, H., Hynes, R. O., and Wagner, D. D. (1993) *Cell* **74,** 541–554
37. Tedder, T. F., Steeber, D. A., and Pizcueta, P. (1995) *J. Exp. Med.* **181,** 2259–2264
38. Coxon, A., Rieu, P., Barkalow, F. J., Askari, S., Sharpe, A. H., von Andrian, U. H., Arnaout, M. A., and Mayadas, T. N. (1996) *Immunity* **5,** 653–666
39. Frenette, P. S., Mayadas, T. N., Rayburn, H., Hynes, R. O., and Wagner, D. D. (1996) *Cell* **84,** 563–574
40. Scharffetter-Kochanek, K., Lu, H., Norman, K., van Nood, N., Munoz, F., Grabbe, S., McArthur, M., Lorenzo, I., Kaplan, S., Ley, K., Smith, C. W., Montgomery, C. A., Rich, S., and Beaudet, A. L. (1998) *J. Exp. Med.* **188,** 119–131
41. Ding, Z. M., Babensee, J. E., Simon, S. I., Lu, H., Perrard, J. L., Bullard, D. C., Dai, X. Y., Bromley, S. K., Dustin, M. L., Entman, M. L., Smith, C. W., and Ballantyne, C. M. (1999) *J. Immunol.* **163,** 5029–5038
42. Robinson, S. D., Frenette, P. S., Rayburn, H., Cummiskey, M., Ullman-Culleré, M., Wagner, D. D., and Hynes, R. O. (1999) *Proc. Natl. Acad. Sci. U.S.A.* **96,** 11452–11457
43. Forlow, S. B., White, E. J., Barlow, S. C., Feldman, S. H., Lu, H., Bagby, G. J., Beaudet, A. L., Bullard, D. C., and Ley, K. (2000) *J. Clin. Invest.* **106,** 1457–1466
44. Forlow, S. B., and Ley, K. (2001) *Am. J. Physiol. Heart Circ. Physiol.* **280,** H634–H641
45. Collins, R. G., Jung, U., Ramirez, M., Bullard, D. C., Hicks, M. J., Smith, C. W., Ley, K., and Beaudet, A. L. (2001) *Blood* **98,** 727–735
46. Forlow, S. B., Foley, P. L., and Ley, K. (2002) *FASEB J.* **16,** 1488–1496
47. Stark, M. A., Huo, Y., Burcin, T. L., Morris, M. A., Olson, T. S., and Ley, K. (2005) *Immunity* **22,** 285–294
48. Smith, E., Zarbock, A., Stark, M. A., Burcin, T. L., Bruce, A. C., Foley, P., and Ley, K. (2007) *J. Immunol.* **179,** 8274–8279
49. Lekstrom-Himes, J. A., and Gallin, J. I. (2000) *N. Engl. J. Med.* **343,** 1703–1714
50. Etzioni, A. (2007) *Adv. Exp. Med. Biol.* **601,** 51–60
51. Ley, K., Laudanna, C., Cybulsky, M. I., and Nourshargh, S. (2007) *Nat. Rev. Immunol.* **7,** 678–689
52. Kuijpers, T. W., Tool, A. T., van der Schoot, C. E., Ginsel, L. A., Onderwater, J. J., Roos, D., and Verhoeven, A. J. (1991) *Blood* **78,** 1105–1111
53. Bornfeldt, K. E., Graves, L. M., Raines, E. W., Igarashi, Y., Wayman, G., Yamamura, S., Yatomi, Y., Sidhu, J. S., Krebs, E. G., and Hakomori, S. (1995) *J. Cell Biol.* **130,** 193–206
54. Okamoto, H., Takuwa, N., Yokomizo, T., Sugimoto, N., Sakurada, S., Shigematsu, H., and Takuwa, Y. (2000) *Mol. Cell. Biol.* **20,** 9247–9261
55. Ishii, M., Kikuta, J., Shimazu, Y., Meier-Schellersheim, M., and Germain, R. N. (2010) *J. Exp. Med.* **207,** 2793–2798
56. Liao, J. J., Huang, M. C., and Goetzl, E. J. (2007) *J. Immunol.* **178,** 5425–5428
57. McKenzie, B. S., Kastelein, R. A., and Cua, D. J. (2006) *Trends Immunol.* **27,** 17–23
58. Xia, P., Wang, L., Moretti, P. A., Albanese, N., Chai, F., Pitson, S. M., D'Andrea, R. J., Gamble, J. R., and Vadas, M. A. (2002) *J. Biol. Chem.* **277,** 7996–8003
59. Niessen, F., Schaffner, F., Furlan-Freguia, C., Pawlinski, R., Bhattacharjee, G., Chun, J., Derian, C. K., Andrade-Gordon, P., Rosen, H., and Ruf, W. (2008) *Nature* **452,** 654–658
60. Baker, D. A., Barth, J., Chang, R., Obeid, L. M., and Gilkeson, G. S. (2010) *J. Immunol.* **185,** 2570–2579
61. Snider, A. J., Kawamori, T., Bradshaw, S. G., Orr, K. A., Gilkeson, G. S., Hannun, Y. A., and Obeid, L. M. (2009) *FASEB J.* **23,** 143–152
62. Olivera, A., Eisner, C., Kitamura, Y., Dillahunt, S., Allende, L., Tuymetova, G., Watford, W., Meylan, F., Diesner, S. C., Li, L., Schnermann, J., Proia, R. L., and Rivera, J. (2010) *J. Clin. Invest.* **120,** 1429–1440
63. Puneet, P., Yap, C. T., Wong, L., Lam, Y., Koh, D. R., Moochhala, S., Pfeilschifter, J., Huwiler, A., and Melendez, A. J. (2010) *Science* **328,** 1290–1294
64. Michaud, J., Im, D. S., and Hla, T. (2010) *J. Immunol.* **184,** 1475–1483
65. Alvarez, S. E., Harikumar, K. B., Hait, N. C., Allegood, J., Strub, G. M., Kim, E. Y., Maceyka, M., Jiang, H., Luo, C., Kordula, T., Milstien, S., and Spiegel, S. (2010) *Nature* **465,** 1084–1088
66. Candelore, M. R., Wright, M. J., Tota, L. M., Milligan, J., Shei, G. J., Bergstrom, J. D., and Mandala, S. M. (2002) *Biochem. Biophys. Res. Commun.* **297,** 600–606
67. Gräler, M. H., Bernhardt, G., and Lipp, M. (1998) *Genomics* **53,** 164–169
68. Regard, J. B., Sato, I. T., and Coughlin, S. R. (2008) *Cell* **135,** 561–571
69. Wang, W., Graeler, M. H., and Goetzl, E. J. (2005) *FASEB J.* **19,** 1731–1733
70. McVerry, B. J., and Garcia, J. G. (2005) *Cell. Signal.* **17,** 131–139
71. Adamson, A. S., Collins, K., Laurence, A., and O'Shea, J. J. (2009) *Curr. Opin. Immunol.* **21,** 161–166
72. Lee, H., Deng, J., Kujawski, M., Yang, C., Liu, Y., Herrmann, A., Kortylewski, M., Horne, D., Somlo, G., Forman, S., Jove, R., and Yu, H. (2010) *Nat. Med.* **16,** 1421–1428
73. Alonzi, T., Maritano, D., Gorgoni, B., Rizzuto, G., Libert, C., and Poli, V. (2001) *Mol. Cell. Biol.* **21,** 1621–1632